Investigating the Nature of IGR J17454-2919 Using X-Ray and Near-Infrared Observations

Paizis, A.; Nowak, M. A.; Rodriguez, J.; Segreto, A.; Chaty, S.; Rau, A.; Chenevez, Jérôme; Del Santo, M.; Greiner, J.; Schmidl, S.

Published in:
Astrophysical Journal

Link to article, DOI:
10.1088/0004-637x/808/1/34

Publication date:
2015

Document Version
Publisher's PDF, also known as Version of record

The Astrophysical Journal, 808:34 (9pp), 2015 July 20 doi:10.1088/0004-637X/808/1/34

INVESTIGATING THE NATURE OF IGR J17454–2919 USING X-RAY AND NEAR-INFRARED OBSERVATIONS

A. Paizis[1], M. A. Nowak[2], J. Rodriguez[3], A. Segreto[4], S. Chaty[3,5], A. Rau[6], J. Chenevez[7], M. Del Santo[4], J. Greiner[6], and S. Schmidl[8]

[1] Istituto Nazionale di Astrofisica, INAF-IASF, Via Bassini 15, I-20133 Milano, Italy; ada@iasf-milano.inaf.it
[2] Massachusetts Institute of Technology, Kavli Institute for Astrophysics, Cambridge, MA 02139, USA; mnowak@space.mit.edu
[3] AIM—Astrophysique, Instrumentation et Modélisation (UMR-E 9005 CEA/DSM-CNRS-Université Paris Diderot) Irfu/Service d'Astrophysique, Centre de Saclay F-91191 Gif-sur-Yvette Cedex, France
[4] Istituto Nazionale di Astrofisica, IASF Palermo, Via U. La Malfa 153, I-90146 Palermo, Italy
[5] Institut Universitaire de France, 103, boulevard Saint-Michel, F-75005 Paris, France
[6] Max-Planck-Institute for Extraterrestrial Physics, D-85741 Garching, Germany
[7] National Space Institute, Technical University of Denmark, Elektrovej 327-328, DK-2800 Kgs Lyngby, Denmark
[8] Thüringer Landessternwarte Tautenburg, Sternwarte 5, D-07778 Tautenburg, Germany
Received 2015 February 25; accepted 2015 May 29; published 2015 July 16

ABSTRACT

IGR J17454−2919 is a hard X-ray transient discovered by *INTEGRAL* on 2014 September 27. We report on our 20 ks *Chandra* observation of the source, performed about five weeks after the discovery, as well as on *INTEGRAL* and *Swift* long-term monitoring observations. X-ray broad-band spectra of the source are compatible with an absorbed power law, $\Gamma \sim 1.6$–1.8, $N_H \sim (10$–$12) \times 10^{22}$ cm^{-2}, with no trace of a cut-off in the data up to about 100 keV, and with an average absorbed 0.5–100 keV flux of about $(7.1$–$9.7) \times 10^{-10}$ erg cm^{-2} s^{-1}. With *Chandra*, we determine the most accurate X-ray position of IGR J17454−2919, $\alpha_{J2000} = 17^h45^m27^s.69$, $\delta_{J2000} = -29°19'53''.8$ (90% uncertainty of $0''.6$), consistent with the NIR source 2MASS J17452768–2919534. We also include NIR investigations from our observations of the source field on 2014 October 6 with GROND. With the multi-wavelength information at hand, we discuss the possible nature of IGR J17454−2919.

Key words: accretion, accretion disks – binaries: close – stars: individual (IGR J17454–2919) – X-rays: binaries

1. INTRODUCTION

The bulge of our Galaxy contains a variety of high-energy transient and persistent sources. It is a unique environment where we can study a wide range of X-ray intensities, down to the fainter levels. Quantifying the spatial distribution, activity, and properties of these sources is essential for population studies and hence for understanding the evolution of our own Galaxy. Instruments with large fields of view and high sensitivity in the hard X-ray energy band, which is less contaminated by the numerous soft X-ray emitting stars, are essential ingredients for such a study. In this respect, the *INTEGRAL* observatory (Winkler et al. 2003, 2011), with its regular monitoring and deep observations of the Galactic Center, has offered a fundamental contribution (e.g., Kuulkers et al. 2007; Revnivtsev et al. 2008; Bird et al. 2010; Krivonos et al. 2012; Lutovinov et al. 2013).

On 2014 September 27, *INTEGRAL* discovered the new hard X-ray transient source IGR J17454−2919 (Chenevez et al. 2014b). The source, less than $24'$ from the Galactic Center, was detected by both JEM–X detectors (Lund et al. 2003) in mosaic images obtained from observations during *INTEGRAL* revolution 1460 (2014 September 27–30). The reported JEM–X average fluxes were 6.5 ± 1 mCrab (3–10 keV) and 8.2 ± 1.7 mCrab (10–25 keV). The source was not detected in previous observations of the region, with a 5σ 3–25 keV upper limit of about 1 mCrab. Chenevez et al. (2014b) also report on a *Swift* 2 ks follow-up observation on 2014 October 2. IGR J17454−2919 was clearly visible, $\alpha_{J2000} = 17^h45^m28^s$, $\delta_{J2000} = -29°19'55''$ (90% confidence error of $5''$), only $10''$ from the JEM–X position.

Later on, Chenevez et al. (2014a) reported that the source flux, observed by *INTEGRAL*/JEM–X on 2014 October 18–20, had increased by about a factor of two with respect to the previous observations, reaching a flux of 10 ± 1 mCrab in 3–10 keV and 15 ± 2 mCrab in 10–25 keV.

On 2014 October 10, *NuSTAR* (Harrison et al. 2013) observed IGR J17454−2919 for a total of about 29 ks (Tendulkar et al. 2014). The energy spectrum could be well described by an absorbed power law ($N_H = 3.3 \pm 0.6 \times 10^{22}$ cm^{-2}, $\Gamma = 1.46 \pm 0.06$) with an exponential cut-off (>100 keV) and a broad, asymmetric, iron emission line. The unabsorbed 3–79 keV flux was 3.96×10^{-10} erg cm^{-2} s^{-1}, corresponding to an isotropic luminosity of 3×10^{36} erg s^{-1} at 8 kpc. Similar to JEM–X (Chenevez et al. 2014b), the 3–79 keV light curve did not show any evidence for bursts or pulsations. Tendulkar et al. (2014) noted a 14% drop in the count rate over the course of their observation, with 25 ± 3% rms variability in the form of a power density spectrum (PDS) described by a zero frequency centered Lorentzian with 2 Hz width and peaking at 1 Hz. Additional power in the PDS was seen at low frequencies in the form of a power law. According to the authors, the hard power-law index, high-energy cut-off, and level of variability are consistent with IGR J17454−2919 being an accreting black hole (BH) in the hard state, though the possibility of a low magnetic field neutron star (NS) cannot be ruled out.

On 2014 November 3, we observed IGR J17454−2919 with *Chandra*/HETGS for 20 ks. Our *Chandra*-based position was reported in Paizis et al. (2015) as $\alpha_{J2000} = 17^h45^m27^s.69$, $\delta_{J2000} = -29°19'53''.8$ (90% uncertainty of $0''.6$). This position ($2''.4$

away from the *Swift*/XRT one) is consistent with the near-infrared (NIR) source 2MASS J17452768–2919534.

On 2015 February 16–17, *INTEGRAL* observed again the Galactic Center and Boissay et al. (2015) reported the non-detection of IGR J17454–2919, with an estimated 5σ upper limit on the source flux of 4 mCrab in the 3–10 keV energy band and of 2 mCrab in the 10–20 keV energy band.

At the time of this writing, the nature of IGR J17454–2919 has yet to be unveiled. In this paper we present the results of our *Chandra* observation as well as long-term *INTEGRAL* and *Swift* observations, to place our *Chandra* observation in the source emission context, as well as to obtain a broad-band source coverage. We also report on archival and new NIR observations of the source taken during the outburst.

2. OBSERVATIONS AND DATA ANALYSIS

2.1. Chandra Data

We observed IGR J17454–2919 for 20 ks with *Chandra* on 2014 November 3, between UT 00:05 and 06:17 (MJD 56964.0–56964.26, Observation ID 15744) with the HETGS (Canizares et al. 2000).

Throughout this work we shall consider data from the 0th spectral order for source position extraction, and from the $\pm$1st orders for spectral extraction. Higher spectral orders have very low count rates and thus shall be ignored, while the 0th order spectrum will not be considered in the spectral analysis as it severely suffers from pileup. The data were analyzed in a standard manner, using the CIAO version 4.6 software package and *Chandra* CALDB version 4.6.3.

To increase the signal-to-noise ratio, we have merged the $\pm$ 1st orders in a single first order Medium Energy Grating (MEG) spectrum and a single first order High Energy Grating (HEG) spectrum. Starting from 0.5 and 0.7 keV in MEG and HEG, respectively, the data were grouped to have 7σ bins (for the investigation of discrete features) and 14σ (for the joint *Chandra*/*Swift* spectra). Spectra were fitted using XSPEC version 12.7.0. Only the results from the latter grouping (consistent with the former) are shown in the paper.

Our *Chandra* observation revealed another bright source located slightly further than 18′ from our target source. Basic results on the source are also given in Section 3.1.2.

2.2. Swift Data

The *Swift* satellite pointed IGR J17454–2919 five times between 2014 October 11 and 2014 November 2, the latter being one day prior to our *Chandra* observation. The log of the observations is reported in Table 1.

Table 1
Journal of the *Swift*/XRT Observations of IGR J17454–2919

ObsId (#)	Date Start (UTC)	Exposure (s)	XRT mode
00033470002	2014 Oct 11 00:10:17	4640	WT
00033470003	2014 Oct 13 06:56:17	1594	WT
00033470004	2014 Oct 13 04:48:45	4365	PC[a]
00033470006	2014 Oct 23 08:06:21	1673	WT
00033470007	2014 Nov 02 07:52:01	1015	PC

Note.
[a] Spectrum strongly piled up and not used.

The *Swift*/XRT spectra were obtained thanks to the online tool provided by the *Swift* UK center.[9] The complete procedure for product extraction is described in Evans et al. (2009). Note that, as recommended for absorbed sources, we extracted spectra from grade 0 only for the window timing data. We also cross-checked the results by reducing a couple of the observations from the raw data following standard procedures using the HEASOFT software suite (through XSELECT, e.g., Rodriguez et al. 2010, 2011). As the products showed no significant deviations, we used those obtained from the online tool for the spectral fits obtained here. The data were grouped so as to have a minimum of 25 counts per bin and then fitted in XSPEC between 0.6 and 8/10 keV, depending on the quality of the data.

The *Swift*/BAT survey data, retrieved from the HEASARC public archive,[10] cover the period from MJD 56778.2 to 57032.9 (2014 May 1–2015 January 10). Due to solar constraints, no observatory could look at the source after 2014 November and IGR J17454–2919 was not detected in the available *Swift*/BAT data after the solar constraint up to 2015 January 10.

The *Swift*/BAT data were processed using BAT_IMAGER software (Segreto et al. 2010). This ad hoc code, dedicated to the processing of coded mask instrument data, computes all-sky maps and, for each detected source, produces standard products such as light curves and spectra. We note that the code takes into account the cross-contamination between sources in the field of view. This is essential in crowded fields such as that of IGR J17454–2919 which has two nearby sources, 1A 1742–294, 13′ away, and AX J1745.6–2901, 18′ away (see also Cusumano et al. 2015 for another application of the decontamination process). The *Swift*/BAT spectra were analyzed in XSPEC between 15 and 150 keV.

2.3. INTEGRAL Data

IGR J17454–2919 has been in the *INTEGRAL* field of view during the observations of the Galactic Center (ID 1120027) and of the Galactic Bulge region[11] (ID 1120001). The third set of observations covering the source (ID 1020021) consists of proprietary data and is not included in this work. A complete study of these *INTEGRAL* data is out of the scope of this paper, however, to get a sense of the broad-band long-term behavior of the source, we have analyzed the IBIS/ISGRI and JEM–X[12] data (Lebrun et al. 2003; Lund et al. 2003, respectively) starting from revolution 1446 (2014 August 18, 01:17:28 UT, MJD 56887.05, about 40 days prior to the reported discovery) up to revolution 1470 (2014 October 28, 15:42:00 UT, MJD 56958.65), the latest dates compatible with solar constraints. The first *INTEGRAL* observation of the Galactic Center occurred again on 2015 February 16–17, during which IGR J17454–2919 was not detected (Boissay et al. 2015).

A standard analysis using version 10.1 of the Off-line Scientific Analysis (OSA) software was performed on the pointings where the source was simultaneously in the field of view of IBIS/ISGRI and JEM–X.

[9] http://www.swift.ac.uk/user_objects/
[10] http://swift.gsfc.nasa.gov/archive/
[11] http://integral.esac.esa.int/BULGE/
[12] Results are given for JEM–X1 and JEM–X2 combined.

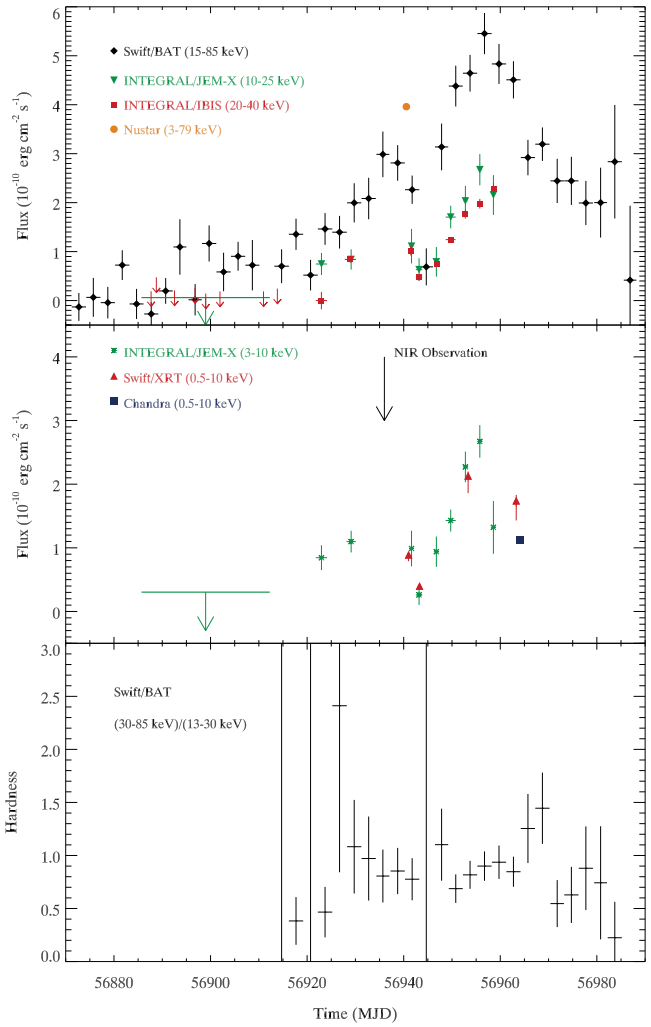

Figure 1. 2014 outburst of IGR J17454−2919 as seen by different high-energy missions. The date of our GROND NIR observation is marked as a black vertical arrow in the middle panel. See Section 3 for details.

2.4. Near-infrared Data

With our *Chandra* position of IGR J17454−2919 at hand, we searched for candidate counterparts in several NIR surveys and obtained new optical/NIR observations of the source field during the outburst.

The position of IGR J17454−2919 had been observed on 2010 August 15 by the VVV Survey (Minniti et al. 2010), on 2006 July 18 during UKIDSS[13] (Lawrence et al. 2007), and also on 1998 July 2 as part of 2MASS (Skrutskie et al. 2006).

Furthermore, we observed IGR J17454−2919 during the outburst with the 7 channel imager Gamma-ray burst Optical NIR Detector (GROND, Greiner et al. 2008) at the MPG 2.2 m telescope at ESO La Silla Observatory at UT 00:31 on 2014 October 6 (MJD 56936.0). GROND observes in the four optical and three near-IR bands simultaneously. Because of the severe Galactic foreground reddening ($A_V \sim 44$, $A_J \sim 12$), we consider here only the J, H, and K_s bands. The total integration time in each band was 10.7 minutes and the average seeing was 1.″3. The GROND data were reduced and analyzed with the standard tools and methods described in Krühler et al. (2008). Here, the J,H, and K_s photometry was measured from 1.″3 apertures and calibrated relative to point-like field sources from the UKIDSS DR10 (Lawrence et al. 2012).

[13] The UKIDSS project is defined in Lawrence et al. (2012). UKIDSS uses the UKIRT Wide Field Camera (Casali et al. 2007). The photometric system is described in Hewett et al. (2006), and the calibration is described in Hodgkin et al. (2009). The pipeline processing and science archive are described in Hambly et al. (2008). We have used data from the tenth data release, which is described in detail in Lawrence et al. (2012).

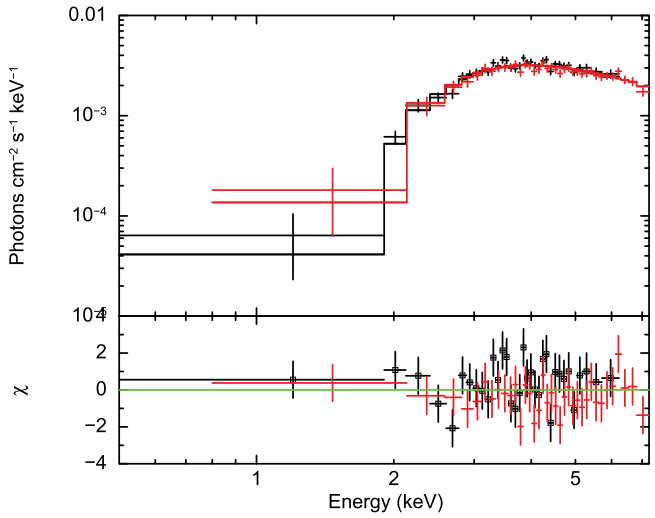

Figure 2. Merged ±1st order MEG (black, box symbol in the residuals) and HEG (red) spectra with best-fit `tbabs*po` model. See Table 2 and Section 3.1.1.

3. RESULTS

A summary of all the data discussed in this work is shown in Figure 1 where the overall 2014 outburst of IGR J17454−2919 can be seen.

The upper panel depicts the hard *X-ray* behavior of IGR J17454−2919 with results from *INTEGRAL*/JEM–X (10–25 keV flux; green downward triangles), *INTEGRAL*/IBIS (20–40 keV flux; red squares) and *Swift*/BAT (15–85 keV flux; black solid diamonds, 3 day bins). The *NuStar* unabsorbed 3–79 keV flux (yellow circle; Tendulkar et al. 2014) is also shown here.

The middle panel shows the *soft X-ray* behavior with results from *INTEGRAL*/JEM–X (absorbed 3–10 keV flux; green asterisks), *Swift*/XRT (absorbed 0.5–10 keV flux; red triangles), *Chandra*/HETGS (absorbed 0.5–10 keV flux; blue squares). The time of our NIR GROND observation is marked by the black vertical arrow. As it can be seen, it occurred during the first peak of the outburst of IGR J17454−2919, as traced by *Swift*/BAT (upper panel).

The lower panel is the hardness ratio evolution computed with *Swift*/BAT in 30–85 keV versus 15–30 keV.

3.1. Chandra Results

3.1.1. Chandra Position, Variability, and Spectra of IGR J17454−2919

Given the brightness of the source, the 0th order image is piled up, hence the resulting shape of the point-spread function (PSF) is distorted and no longer exactly point-like. This renders the precise centroid position of the source more difficult to locate. For this reason, the source location was determined by intersecting the readout streak with the grating arms. This was accomplished with the `findzo` algorithm,

which is used for determining the 0th order position when a readout streak is detected (and hence pileup is affecting the 0th order image), as in our case.

The X-ray position obtained is $\alpha_{J2000} = 17^h45^m27^s.69$, $\delta_{J2000} = -29°19'53''.8$, as reported in Paizis et al. (2015). Since the statistical error is smaller than the absolute position accuracy of *Chandra*, $0''.6$ at 90% uncertainty,[14] we attribute to the position found a 90% uncertainty of $0''.6$.

The *Chandra* light curve of IGR J17454–2919, similar to what was reported by Chenevez et al. (2014b) and Tendulkar et al. (2014), showed no evidence for bursts or pulsations on the timescales accessible to our *Chandra* observation, i.e., ≈4–10,000 s (twice a *Chandra* time bin to half the observation).

The *Chandra* spectrum of IGR J17454–2919 can be well fit by an absorbed (`tbabs`) power law ($N_H \sim 12 \times 10^{22}$ cm^{-2}, and photon index $\Gamma \sim 1.6$) with an average absorbed 2–8 keV flux of about 1×10^{-10} erg cm^{-2} s^{-1}. Figure 2 shows the best fit we obtained with the absorbed power-law model, while Table 2 shows the obtained parameters.

In the fit, and throughout the paper, we have used an improved model for the absorption of X-rays in the ISM by Wilms et al. (2000).[15] Such a model results in higher column densities with respect to, e.g., the `wabs` model by Morrison & McCammon (1983). For comparison, using the `wabs` model, the following is obtained: $N_H = (8.2 \pm 0.7) \times 10^{22}$ cm^{-2}, and photon index $\Gamma = 1.6 \pm 0.17$.

3.1.2. The Second Source in the Chandra Field of View: AX J1745.6–2901

Our *Chandra* observation revealed another bright source located ∼18′ from our target source.[16] At this off-axis angle, the *Chandra* PSF becomes very extended and obtains an elliptical shape. The image of this source appears as an ellipse with semimajor/semi-minor axes of approximately $1'.1/0'.7$, respectively, with shadows of the mirror support structures clearly visible in the PSF. The intersections of these shadow structures occur within $2''$ of $\alpha_{J2000} = 17^h45^m35^s.44$, $\delta_{J2000} = -29°01'33''.6$ (J2000), which is the location of a known transient, the bursting NS AX J1745.6–2901 (see Muno et al. 2004; Degenaar & Wijnands 2009 and references therein).

We extracted the 0th order spectrum for this source using the CIAO `specextract` tool (taking the background from a nearby $0'.7$ circular region). Binning the spectrum to a signal-to-noise per channel of 8 and noticing the 2–8 keV region, the spectrum is well fit ($\chi^2 = 224.6$ for 222 degrees of freedom) by an absorbed, $N_H = (34 \pm 2) \times 10^{22}$ cm^{-2} power law ($\Gamma = 1.96 \pm 0.14$). Error bars are 90% confidence for one interesting parameter. This N_H value is 50% higher than the value reported by Degenaar & Wijnands (2009); however, they do not specify the absorption model used.

The fitted, unabsorbed 2–10 keV luminosity is 6.1×10^{36} erg cm^{-2} s^{-1}, assuming isotropic emission at a distance of 8 kpc. This would place this outburst of AX J1745.6–2901 at the same level as the brightest of the four historical outbursts discussed by Degenaar & Wijnands (2009) with the other outbursts being approximately 6–30 times fainter.

We searched the source light curve for evidence of variability (there is an 8.4 hr period known from eclipses), including any evidence of type-I bursts, but no statistically significant variability was found on any timescale accessible to this *Chandra* observation (≈4–10,000 s).

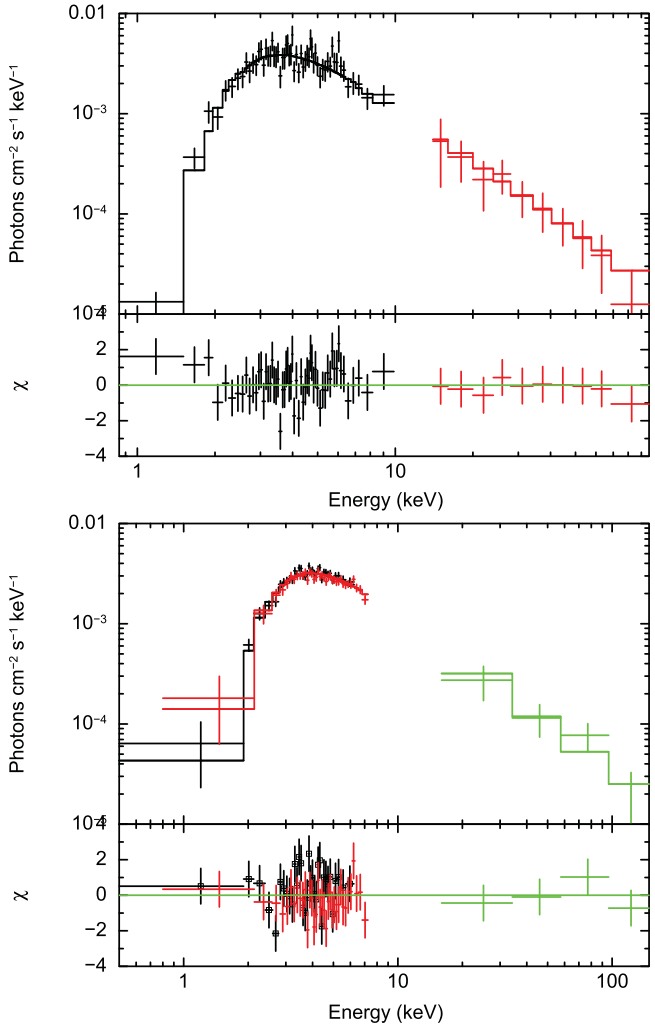

Figure 3. Upper panel: *Swift*/XRT+BAT observation of IGR J17454–2919 (November 2, ObsID 00033470007) and best-fit model `tbabs*po`; see Table 2 and Section 3.3.1. Lower panel: joint *Chandra-Swift*/BAT spectra of IGR J17454–2919 (November 3). Merged ±1st order MEG (black), HEG (red), and *Swift*/BAT (green) spectra with best-fit `tbabs*po` model; see Table 2 and Section 3.3.2.

3.2. Swift Results on IGR J17454–2919

3.2.1. Swift/XRT Results

Excluding the severely piled up observation 00033470004 (see Table 1), we have extracted *Swift*/XRT spectra for the remaining four observations. All spectra could be well fit by an absorbed power law. The obtained fluxes are shown in Figure 1, middle panel. During three of these four observations (first, third, and fourth, chronologically), the source did not show any relevant spectral evolution although the source flux doubled

[14] http://cxc.harvard.edu/cal/ASPECT/celmon/

[15] In XSPEC terminology: `tbabs` with `xsect vern` and `abund wilm`.

[16] We note that this source does not contaminate the results we obtain for IGR J17454–2919 in hard X-rays, with either *INTEGRAL*/IBIS-JEM–X or *Swift*/BAT. Indeed, for *INTEGRAL*, the source is farther than the intrinsic instrumental angular resolution (12′ for IBIS and 3′ for JEM–X), while for BAT source cross-contamination is taken care of by the code used (see Section 2.2).

Table 2
Fit to IGR J17454–2919 Spectra: `tbabs*po`

Spectra	N_H[a] (10^{22} cm^{-2})	Γ (10^{-10} erg cm^{-2} s^{-1})	Average U_Flux (10^{-10} erg cm^{-2} s^{-1})	Average Flux (10^{36} erg s^{-1})	Average Luminosity	Red χ^2/ dof
Chandra/HETGS	$12.1^{+0.8}_{-1.1}$	1.6±0.2	2.0[b]	1.1[c]	0.9[d]	1.05/66
Swift/(XRT+BAT)	$10.5^{+1.2}_{-1.1}$	1.8±0.1	9.7[e]	7.1[f]	5.4[g]	0.87/66
Chandra/HETGS+*Swift*/BAT	$11.9^{+1.1}_{-1.0}$	1.6±0.2	11.7[e]	9.7[f]	7.4[g]	1.03/69

Notes. Error bars are 90% confidence level for one parameter. *Chandra* spectra are shown in Figure 2 and discussed in Section 3.1.1. *Swift*/(XRT+BAT) spectra are shown in Figure 3, upper panel, and discussed in Section 3.3.1 while *Chandra*–*Swift*/BAT spectra are shown in Figure 3, lower panel, and discussed in Section 3.3.2.
[a] In the fit we have used an improved model for the absorption of X-rays in the interstellar medium by Wilms et al. (2000).
[b] Unabsorbed 2–8 keV flux.
[c] Absorbed 2–8 keV flux.
[d] Absorbed 2–8 keV luminosity, assuming a distance of 8 kpc.
[e] Unabsorbed 0.5–100 keV flux.
[f] Absorbed 0.5–100 keV flux.
[g] Absorbed 0.5–100 keV luminosity, assuming a distance of 8 kpc.

with the spectral slope remaining around $\Gamma = 1.5\pm0.3$ and an absorption within the interval $N_H \sim (7.5\text{–}10.7) \times 10^{22}$ cm^{-2}. The second observation, 00033470003 occurred on 2014 October 13 (MJD = 56943.28), resulted in a very poorly constrained fit ($\Gamma = 2.1^{+1.4}_{-1.0}$ and $N_H = 8.5^{+6.5}_{-3.7} \times 10^{22}$ cm^{-2}) since the source experiences a flux drop, as also detected by *INTEGRAL* and *Swift*/BAT (Figure 1).

3.2.2. Swift/BAT Results

Due to its extremely wide field of view, *Swift*/BAT has nicely monitored IGR J17454–2919. The all-outburst *Swift*/BAT light curve (3 day bins) can be seen in Figure 1, upper panel, while the hardness ratio in the bands 30–85 keV versus 15–30 keV is shown in Figure 1, lower panel.

A complete study of all the *Swift*/BAT data is beyond the scope of the paper, but we have extracted *Swift*/BAT spectra for three time intervals: the first one corresponding to *Swift*/XRT ObsID 00033470007 (see Table 1, MJD 56963.3, November 2, *Swift*/BAT exposure of about 87 ks) about a day prior to our *Chandra* data, the second *simultaneous* with our *Chandra* observation (MJD 56964.0, November 3, ∼17 ks), and the third covering the outburst peak of IGR J17454–2919, from October 20 to November 4 (MJD 56950–56965, roughly the highest five bins in Figure 1, 172 ks).

The three *Swift*/BAT spectra could be well fit by a simple power law with $\Gamma = 1.9\pm0.5$ (November 2), $\Gamma = 1.3 \pm 0.8$ (November 3) and $\Gamma = 1.9\pm0.1$ (peak). Though the second result ($\Gamma = 1.3 \pm 0.8$) appears to suggest a hardening of IGR J17454–2919, the result is not statistically significant and the slopes overlap.

In the next section we use the *Swift*/BAT spectra to investigate the broad-band behavior of IGR J17454–2919.

3.3. Broad-band Results of IGR J17454–2919

3.3.1. Swift/(XRT+BAT) Observation (November 2)

The simultaneous *Swift*/(XRT+BAT) spectrum of IGR J17454–2919 as obtained from November 2 (see Table 1) can be well fit by an absorbed power law ($N_H \sim 10.5 \times 10^{22}$ cm^{-2} and photon index $\Gamma \sim 1.8$) with an average absorbed 0.5–100 keV flux of about 7.1×10^{-10} erg cm^{-2} s^{-1}. Figure 3, upper panel, shows the best fit we obtained with the absorbed power-law model, while Table 2 shows the obtained parameters. There is clearly no need for a power-law cut-off energy in the data.

3.3.2. Chandra-Swift/BAT Observation (November 3 and Peak)

As visible in Figure 1, our *Chandra* observation is simultaneous with a *Swift*/BAT coverage. Hence to obtain broad-band information on the source, we performed a joint *Chandra-Swift*/BAT spectral fitting of the simultaneous data.

The data can be well fit by an absorbed power law ($N_H \sim 11.9 \times 10^{22}$ cm^{-2} and photon index $\Gamma \sim 1.6$) with an average absorbed 0.5–100 keV flux of about 9.7×10^{-10} erg cm^{-2} s^{-1}. Figure 3, lower panel, shows the best fit we obtained with the absorbed power-law model, while Table 2 shows the obtained parameters.

Similar to the previous case, there is no trace of a high-energy cut-off in the data.

From Figure 1 it is possible to see that our *Chandra* observation occurred at a *Swift*/BAT (15–85 keV) flux similar to the *NuSTAR* one. Hence to compare the results, we fitted our broad-band *Chandra-Swift*/BAT spectra with the same model used by Tendulkar et al. (2014), i.e., a cut-off power-law with absorbing model (`tbabs`; S. P. Tendulkar, private communication) and abundances by Anders & Grevesse (1989), instead of the ones used up until now by Wilms et al. (2000). We obtained: $N_H = 7.7 \pm 0.7 \times 10^{22}$ cm^{-2}, $\Gamma = 1.57^{+0.07}_{-0.18}$, and a cut-off energy of $E_{\rm cut} > 80$ keV. Compared to the results by Tendulkar et al. (2014) ($N_H = 3.3 \pm 0.6 \times 10^{22}$ cm^{-2}, $\Gamma = 1.46 \pm 0.06$ and $E_{\rm cut} > 100$ keV), we see that while the power-law slope and cut-off energy are comparable, the absorbing column density is about a factor of two different.

As a final check, we fit the *Chandra* data with the peak *Swift*/BAT spectrum (with the *peak* defined in Section 3.2.2 i.e., from October 20 to November 4, roughly the highest five bins in Figure 1), in an attempt to improve the fit quality with the better *Swift*/BAT statistics, for there is an overlap, though the data are not exactly simultaneous. Similar to the previous cases, there is no significant detection of a cut-off in the spectrum with energy $E_{\rm cut} > 80$ keV.

3.4. INTEGRAL

During the discovery outburst, the source was never detected in a single *INTEGRAL* pointing (∼2 ks) and several pointings needed to be stacked to increase the sensitivity with longer

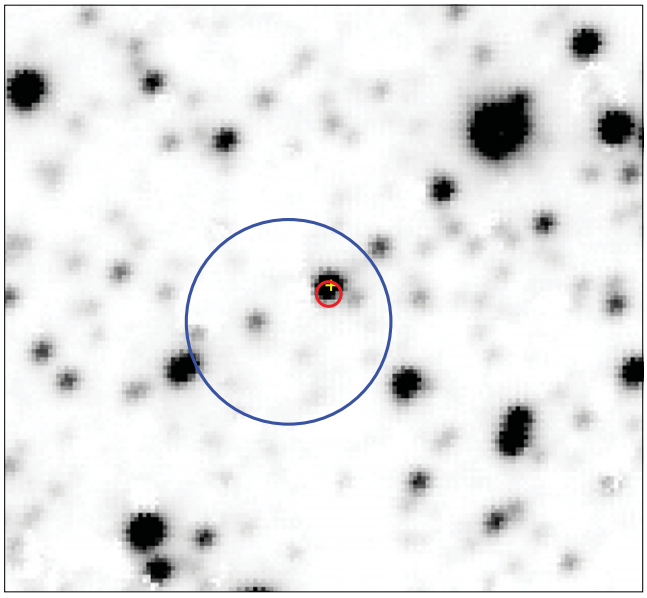

Figure 4. Archival UKIDSS K_s image of the field around IGR J17454–2919. The *Swift*/XRT 90% error circle (5″ in blue, Chenevez et al. 2014b) and *Chandra* 90% error circle (0″.6 in red, this work) are shown. 2MASS J17452768–2919534 is indicated with a yellow cross. North is up and east is left. See Section 3.5.

exposures. Therefore, we have built mosaic images with the IBIS/ISGRI and JEM–X1+2 instruments to obtain average flux measurements for each *INTEGRAL* revolution. In Figure 1 (upper panel), we show the source flux variations between 20–40 keV (IBIS/ISGRI) and 10–25 keV (JEM–X), while the 3–10 keV (JEM–X) flux variations are shown in the middle panel. In the case of JEM–X, upper limits in Figure 1 are from the total combined JEM–X mosaic with the deepest exposure available prior to the onset of the outburst and are at 5σ, while for IBIS/ISGRI the upper limits are given per revolution and are at 3σ.

Inspection of our all-public IBIS/ISGRI archive (2002 October–2014 March; Paizis et al. 2013, 17–50 keV) for previous unnoticed outbursts from IGR J17454–2919 shows that during the 35.2 Ms (good IBIS/ISGRI time) in which IGR J17454–2919 was in the IBIS/ISGRI field of view (source position within 15° from the pointing coordinates), the source has never been detected at a single pointing level (~2 ks), implying that IGR J17454–2919 was (at best) at the detection limit in IBIS/ISGRI, corresponding to about 20 mCrab in a 2 ks pointing (Krivonos et al. 2010).

3.5. Near-infrared

Figure 4 shows the archival UKIDSS K_s image of the field around IGR J17454–2919. The *Swift*/XRT 90% error circle (5″ in blue, Chenevez et al. 2014b) and *Chandra* 90% error circle (0″.6 in red, this work) are shown. While the *Swift*/XRT position error includes more than one source in the crowded field toward the Galactic Center, our *Chandra* position coincides within the errors with a 2MASS object, 2MASS J17452768–2919534 (indicated with a yellow cross in the map) which makes it the most likely NIR counterpart.

Due to the large Galactic foreground reddening, no optical counterpart is detected in the GROND g', r', i', z' bands. However, the likely 2MASS counterpart is detected in the infrared J, H and K_s bands.

Table 3
GROND, 2MASS, UKIDSS, and VVV Photometry

Band	GROND[a]	2MASS[b]	UKIDSS[b]	VVV[b]
J[c]	16.07 ± 0.08	>16.227	16.587 ± 0.015	16.46 ± 0.02
H	13.10 ± 0.07	13.038 ± 0.065	13.150 ± 0.003	13.12 ± 0.01
K_s	11.37 ± 0.06	11.365 ± 0.024	11.334 ± 0.002	11.37 ± 0.01

Notes.
[a] NIR during source outburst.
[b] Archival NIR catalogs.

A comparison of the GROND, UKIDSS, 2MASS, and VVV[17] photometry (all magnitudes in the Vega System) is presented in Table 3.

The candidate counterpart is constant within the error bars in the K_s band and also constant between GROND, UKIDSS, and VVV in the H band. The J band, however, shows a hint of variability with respect to UKIDSS and the VVV survey. Hence, we conclude that 2MASS J17452768–2919534 underwent a slight brightening in the J band during the X-ray outburst, while it remained constant in the H and K_s bands.

4. DISCUSSION

After the discovery, IGR J17454–2919 underwent an outburst of about 60 days (MJD 56923.7–56983.7, as suggested by the last non-detection in *Swift*/BAT; see Figure 1). Due to solar constraints, however, no observatory could look at the source after 2014 November, so a longer outburst cannot be excluded.

The X-ray light curve of IGR J17454–2919 (Figure 1) shows a double peak with a clear flux decrease seen in all X-ray bands around MJD 56945 (duration ~4–5 days). The obtained spectra during such a dip are too dim to verify a significant variability of the spectral model parameters (see Section 3.2 and Figure 1 lower panel), but the fact that this flux decrement is present in all the X-ray data may suggest that it does not correspond to an important spectral state change, rather to a decrease in the overall flux. Such a decrease may be due to an intrinsic change in mass transfer from the companion in an eccentric orbit (see, e.g., the few, ~2–3, day dip in the X-ray light curve of Cir X–1, Murdin et al. 1980; Shirey et al. 1996), or due to a change of the absorbing medium (dips from intervening matter or eclipses by the donor or by a tilted and/or warped accretion disk, see, e.g., Clarkson et al. 2003 and references therein).

Broad-band spectra of the source are compatible with an absorbed power law ($\Gamma \sim 1.6$–1.8 and $N_H \sim 10$–12×10^{22} cm^{-2}), with no trace of a cut-off in the data. Unlike *NuSTAR* (Tendulkar et al. 2014), we do not see evidence of a broad iron line in our soft X-ray spectra, which is not a surprise considering the significantly larger effective collecting area in the iron domain of *NuSTAR* with respect to *Chandra* and *Swift*/XRT. Using the same model by Tendulkar et al. (2014) to fit our broad-band *Chandra*–*Swift*/BAT spectra, we obtained a significantly different absorbing column density, $N_H = (7.7 \pm 0.7) \times 10^{22}$ cm^{-2} versus their $N_H = (3.3 \pm 0.6) \times 10^{22}$ cm^{-2}. This could imply a real variability in N_H (hence a

[17] We took here default 2″ aperture photometry of the VVV catalog (so-called `jAperMag3`, `hAperMag3`, and `ksAperMag3`), and we also added the uncertainty in the photometric zero-points of 0.01 mag, in quadrature to the cataloged statistical uncertainties.

part of it is local to the system), but we note that the discrepancy could be due to the lack of data below 3 keV and/or to the modeling of the Fe line in the *NuSTAR* data.

The X-ray characteristics of IGR J17454−2919 are typical of a low mass X-ray binary (LMXB) rather than of a high mass X-ray binary (HMXB). Indeed, most HMXBs, apart from the exceptionally few BH HMXBs such as Cyg X–1, have spectra with a very clear cut-off below 40 keV (Coburn et al. 2002), while IGR J17454−2919 has a clear non-attenuated power-law up to 100 keV, as seen in the broad-band spectra presented in the present work. Furthermore, the spectral slope of IGR J17454−2919 is typical of an LMXB in the low–hard state, different from the flatter slope generally seen in HMXBs ($\Gamma \sim 1$).

Regarding the nature of the compact object in the binary system, we note that up until now no pulsations or type-I X-ray bursts, which would point to the presence of an NS in the system, have been detected (this work; Chenevez et al. 2014a, 2014b; Tendulkar et al. 2014). Furthermore, the spectral analysis and long-term light curve investigated in this work do not seem to strongly favor the BH option, with respect to the NS. Indeed, the ultra-compact binary and X-ray burster (hence an LMXB with an NS) 4U 1850–087 has shown a similar spectrum to IGR J17454−2919: a non-attenuated power law up to about 100 keV, with a best-fit photon index of $\Gamma = 1.9 \pm 0.1$ and a 2–100 keV luminosity of $\sim 1.5 \times 10^{36}$ erg s^{-1} at 6.8 kpc (Sidoli et al. 2006). This source, observed with *BeppoSAX* and *INTEGRAL*, spent most of the time in this low-luminosity hard state. Its simultaneous *XMM-Newton*/EPIC-*INTEGRAL*/IBIS spectrum required a soft disk emission in addition to the power law ($kT_s = 0.8 \pm 0.1$), but the source had a very low absorbing column density ($N_H = 0.4 \times 10^{22}$ cm^{-2}), whereas in our case N_H, be it local to the system or Galactic, is high and the soft disk component, if any, is most likely hidden and undetected.

The peak flux reached by IGR J17454−2919 during the outburst as seen by *Swift*/BAT in 15–85 keV is $(5.5 \pm 0.4) \times 10^{-10}$ erg cm^{-2} s^{-1} (Figure 1). Placing the source at 8 kpc and assuming the same spectrum as in Table 2, we obtain a corresponding 0.5–100 keV peak luminosity of 9×10^{36} erg s^{-1} (3.5×10^{36} erg s^{-1} at 5 kpc) which is in the range of X-ray binary outbursts (both LMXB and HMXB). In this respect, the peak flux does not allow us to constrain the nature of the source. On the other hand, broad asymmetric iron lines such as the one detected by Tendulkar et al. (2014) are in general typical of accretion disks, hence mainly found in LMXBs (e.g., Ng et al. 2010), whereas in the case of HMXBs, the observed lines have normally a narrow profile (e.g., Vela X–1, GX 301–2, 4U 1700–37), usually interpreted as fluorescence of iron in a wind or circumstellar matter (Rodriguez et al. 2006; Giménez-García et al. 2015).

The large value of the absorption we obtain ($N_H \sim$ 10–12 $\times 10^{22}$ cm^{-2} or $N_H = 8.2 \pm 0.7 \times 10^{22}$ cm^{-2} using `wabs`) is well in excess with respect to the average Galactic value in the source direction, $\sim 1.2 \times 10^{22}$ cm^{-2} (Dickey & Lockman 1990). This could imply that there is an additional contribution from within the system and/or that we are seeing the system at high inclination. Nevertheless, the value obtained with the radio maps by Dickey & Lockman (1990) does not resolve the small scale, $<1'$, non-uniformity of N_H and does not include the possible contribution of molecular hydrogen, probably underestimating the true value. Indeed also the second source in the *Chandra* field of view, AX J1745.6−2901, located $\sim 18'$ from our target source, is heavily obscured with $N_H = (34 \pm 2) \times 10^{22}$ cm^{-2} (average Galactic value in the source direction, $\sim 1.2 \times 10^{22}$ cm^{-2}; Dickey & Lockman 1990) possibly related to the patchy nature of N_H toward the Galactic Center.

Our NIR observations showed that 2MASS J17452768−2919534 underwent a slight brightening in the J band during the X-ray outburst, while it remained constant in the H and K_s bands. This variability detected in the bluer bands rather than in the K_s band could be consistent with an enhanced emission from an accretion disk of an LMXB in which the donor star (or even the jet emission) dominates the NIR flux in H and K_s with an increasing disk contribution at bluer wavelengths (e.g., Charles et al. 2006; Khargharia et al. 2010).

To estimate the extinction toward the source, we modify the relationship of Predehl & Schmitt (1995) to account for the fact that the absorption model of Wilms et al. (2000) used throughout the paper fits neutral columns ≈30% larger than the model used by Predehl & Schmitt (1995). Hence we assume $A_V \sim N_H / 2.7 \times 10^{21}$ cm^{-2} (as in Nowak et al. 2012).

Using the ratio $A_{K_s}/A_V = 0.112$ and $A_J/A_V = 0.282$ (Rieke & Lebofsky 1985), our broad-band observed column density $N_H \sim 11.9 \times 10^{22}$ cm^{-2} translates into an absolute K_s magnitude $M_{K_s} = -8.1$ mag with an assumed distance of 8 kpc ($M_{K_s} = -7.1$ mag at 5 kpc), an absolute J magnitude $M_J = -10.9$ mag ($M_J = -9.9$ mag at 5 kpc) and M_J-$M_{K_s} = -2.8$ mag. The obtained K_s band value is compatible with an M-type companion in the case of a red giant, however, the M_J-M_{K_s} value does not seem to fit with any spectral type (see Figure 1 in Chaty et al. 2002, where $-0.5 < M_J$-$M_{K_s} < +1.5$). Notwithstanding the patchy nature of N_H toward the Galactic Center, it would take an unusually low extinction to match the obtained value to a given spectral type.

We note that similar results also are obtained if we use more recent interstellar extinction laws, such as those by Nishiyama et al. (2009) and Güver & Özel (2009). In both cases, the K_s band indicates an M-type red giant companion (LMXB), whereas M_J-M_{K_s} does not belong to any spectral type (M_J-$M_{K_s} = -3.2$ and −4.45 mag, respectively).

On the other extreme, we could consider that all the absorbing material is local to the accreting compact object alone, while the companion is not enshrouded in it. In this case, as in some *INTEGRAL* highly absorbed HMXBs (e.g., Chaty 2013, and references therein), we estimate the extinction toward the source only using the expected line of sight absorption ($\sim 1.2 \times 10^{22}$ cm^{-2} Dickey & Lockman 1990). This leads to an absolute K_s magnitude $M_{K_s} = -3.9$ mag for an assumed distance of 8 kpc ($M_{K_s} = -2.9$ mag at 5 kpc), compatible with a K-type/M-type red giant companion (LMXB) or a B-type main sequence star (HMXB). Similar to the previous case, the M_J-M_{K_s} value obtained (M_J-$M_{K_s} = +3.6$ mag) does not seem to match any spectral type. Most likely, IGR J17454−2919 lies somewhere in between, with *some* of the absorbing material local to the accreting compact object. Furthermore, part of the M_J-M_{K_s} discrepancy could mean that we are seeing the contribution from the accretion disk (suggesting an LMXB). Indeed, NIR increases up to ∼4–7 mag have been seen in the high–soft state of LMXBs (Charles et al. 2006), and of about 3 mag in the low–hard state (Chaty et al. 2003).

Since IGR J17454−2919 is right in the crowded region of the Galactic Center, it is possible that the associated NIR counterpart discussed up to now is not the correct one, with the real one lying behind our candidate, or within a blend with other bright stars dominating the NIR scene. As a first order estimate, however, we note that in Figure 4 we have about 25 sources comparably bright to IGR J17454−2919 in an area about 790 times that of the *Chandra* error circle, resulting in a low chance coincidence probability of about 3%.

For completeness, we also investigate the active galactic nucleus (AGN) possibility. There are a few examples of AGNs located in the Galactic Plane, and even toward the Galactic Center (Chaty et al. 2008; Zurita Heras et al. 2009; Tomsick et al. 2012). However, no extragalactic object is known to be located within a radius of 30′ from the Galactic Center (SIMBAD), with IGR J17454−2919 being less than 24′ from it. Furthermore, IGR J17454−2919, with its $\sim 2 \times 10^{-10}$ erg cm^{-2} s^{-1} in 20–40 keV (see Figure 1) would place itself among the brightest AGNs detected by *INTEGRAL*. Compared with Beckmann et al. (2009), we see that out of 199 AGNs detected with *INTEGRAL* above 20 keV, only 4 have a flux brighter than 1×10^{-10} erg cm^{-2} s^{-1} in the 20–40 keV: Mrk 421 (BLLac), NGC 4151 (Sy1.5), Cen A (Sy 2), and the Circinus Galaxy (Sy 2). The latter three are Seyfert galaxies and, similar to IGR J17454−2919, are highly absorbed in X-rays, but while in their case this results in a significant infrared K_s emission due to the thermal radiation from the dust (∼4 mag for Cen A and ∼7.5 mag for NGC 4151, Skrutskie et al. 2006), in our case we reach a level of ∼11 mag, much dimmer. On the other hand, this source seems too absorbed to be a blazar AGN (e.g., for Mrk 421, $N_H = 0.08 \times 10^{22}$ cm^{-2} is obtained). Finally, the AGN hypothesis also is discarded by the NIR images since if the X-rays were from an AGN similar to the above, the source would be nearby and thus we would observe an NIR extended source (several arcseconds to even arcminutes, see, e.g., the dimmer IGR J09026−4812 with its 4.″9 semimajor axis in K_S; Zurita Heras et al. 2009). This is clearly not the case in the archival and GROND NIR maps.

5. SUMMARY

On 2014 September 27, *INTEGRAL* discovered the new transient, IGR J17454−2919, 24′ away from the Galactic Center. The outburst lasted at least about 60 days, with a longer monitoring being hampered by solar constraints. We studied the long-term X-ray light curve and broad-band spectra of IGR J17454−2919 using data from three high-energy missions: *Chandra*, *Swift* , and *INTEGRAL*.

The outburst X-ray light curve shows a double peak with a clear ∼4–5 day flux decrease seen in *all* X-ray bands. This may suggest a mass transfer change from the companion in an eccentric orbit or a change of the absorbing medium (e.g., dips from intervening matter, eclipses by the donor or by a tilted and/or warped accretion disk).

The outburst peak flux is $\sim 5.5 \times 10^{-10}$ erg cm^{-2} s^{-1} (15–85 keV) corresponding to a 0.5–100 keV peak luminosity of 9×10^{36} erg s^{-1} at 8 kpc in the range of X-ray binary outbursts. The broad-band spectra of the source are compatible with an absorbed power law ($\Gamma \sim$ 1.6–1.8 and $N_H \sim$ 10–12 $\times 10^{22}$ cm^{-2}), with no trace of a cut-off in the data up to about 100 keV. This is compatible with an LMXB in the low–hard state. The detection of a broad iron line by *NuSTAR* (Tendulkar et al. 2014) strengthens this association. As of the time of this writing, there was no indication of the nature of the compact object (i.e., pulsations or type-I X-ray bursts that would point to an NS).

With *Chandra*, we determined the most accurate X-ray position of IGR J17454−2919, enabling a candidate NIR counterpart search in the crowded field toward the Galactic Center. The X-ray position of IGR J17454−2919 is compatible with the NIR source 2MASS J17452768−2919534. Archival (2MASS, UKIDSS, VVV) and new (GROND) NIR observations of the source taken during the 2014 outburst have been investigated.

The obtained K_s band values are compatible with an K-type/M-type companion in the case of a red giant with a hint of brightening in the J band. This is consistent with an enhanced emission from the accretion disk of an LMXB. Moreover, the M_J-M_{K_s} value does not seem to match any spectral type and this could mean that we are seeing the contribution from the accretion disk, with some of the absorbing material possibly local to the accreting object alone.

It is not straightforward to unveil the nature of this elusive source. However, considering the outburst X-ray properties and the NIR ones, IGR J17454−2919 is most likely an LMXB with no current indication of the nature of the compact object.

We thank the *Chandra* team for their rapid response in scheduling and delivering the observation.

This work is partly based on observations with *INTEGRAL*, an ESA project with instruments and science data center funded by ESA member states, Czech Republic and Poland, and with the participation of Russia and the USA.

This research has made use of the *INTEGRAL* sources page http://irfu.cea.fr/Sap/IGR-Sources/.

Part of the GROND funding (both hardware and personnel) was generously granted from the Leibniz-Prize to Prof. G. Hasinger, Deutsche Forschungsgemeinschaft (DFG) grant HA 1850/28-1. Sebastian Schmidl acknowledges support by the Thüringer Ministerium für Bildung, Wissenschaft und Kultur under FKZ 12010-514. This work is based on data products from observations made with ESO Telescopes at the La Silla or Paranal Observatories under ESO programme ID 179.B-2002.

This publication makes use of data obtained as part of the UKIRT Infrared Deep Sky Survey and of data products from the 2MASS, which is a joint project of the University of Massachusetts and the Infrared Processing and Analysis Center/California Institute of Technology, funded by the National Aeronautics and Space Administration and the National Science Foundation.

A.P. acknowledges the Italian Space Agency financial support *INTEGRAL* ASI/INAF agreement no. 2013-025.R.0. M.A.N. acknowledges support from NASA Grant G04-15027X. J.C. acknowledges financial support from ESA/PRODEX Nr. 90057. J.R. acknowledges funding support from the UnivEarthS Labex program of Sorbonne Paris Cité (ANR-10-LABX-0023 and ANR-11-IDEX-0005-02). A.P. thanks Lara Sidoli and Volker Beckmann for useful discussions. We thank the anonymous referee for the accurate reading of the manuscript.

REFERENCES

Anders, E., & Grevesse, N. 1989, GeCoA, 53, 197
Beckmann, V., Soldi, S., Ricci, C., et al. 2009, A&A, 505, 417
Bird, A. J., Bazzano, A., Bassani, L., et al. 2010, ApJS, 186, 1

Boissay, R., Chevenez, J., Wilms, J., et al. 2015, ATel, 7096
Canizares, C. R., Huenemoerder, D. P., Davis, D. S., et al. 2000, ApJL, 539, L41
Casali, M., Adamson, A., Alves de Oliveira, C., et al. 2007, A&A, 467, 777
Charles, P. A., & Coe, M. J. 2006, in Optical, Ultraviolet, and Infrared Observations of X-ray Binaries, ed. W. Lewin & M. van der Klis (Cambridge: Cambridge Univ. Press), 215
Chaty, S. 2013, AdSpR, 52, 2132
Chaty, S., Haswell, C. A., Malzac, J., et al. 2003, MNRAS, 346, 689
Chaty, S., Mirabel, I. F., Goldoni, P., et al. 2002, MNRAS, 331, 1065
Chaty, S., Rahoui, F., Foellmi, C., et al. 2008, A&A, 484, 783
Chenevez, J., Brandt, S., Budtz-Jorgensen, C., et al. 2014a, ATel, 6530
Chenevez, J., Brandt, S., Budtz-Jorgensen, C., et al. 2014b, ATel, 6602
Clarkson, W. I., Charles, P. A., Coe, M. J., et al. 2003, MNRAS, 339, 447
Coburn, W., Heindl, W. A., Rothschild, R. E., et al. 2002, ApJ, 580, 394
Cusumano, G., Segreto, A., la Parola, V., et al. 2015, MNRAS, 446, 1041
Degenaar, N., & Wijnands, R. 2009, A&A, 495, 547
Dickey, J. M., & Lockman, F. J. 1990, ARA&A, 28, 215
Evans, P. A., Beardmore, A. P., Page, K. L., et al. 2009, MNRAS, 397, 1177
Giménez-García, A., Torrejón, J. M., Eikmann, W., et al. 2015, arXiv:1501.03636
Greiner, J., Bornemann, W., Clemens, C., et al. 2008, PASP, 120, 405
Güver, T., & Özel, F. 2009, MNRAS, 400, 2050
Hambly, N. C., Collins, R. S., Cross, N. J. G., et al. 2008, MNRAS, 384, 637
Harrison, F. A., Craig, W. W., Christensen, F. E., et al. 2013, ApJ, 770, 103
Hewett, P. C., Warren, S. J., Leggett, S. K., & Hodgkin, S. T. 2006, MNRAS, 367, 454
Hodgkin, S. T., Irwin, M. J., Hewett, P. C., & Warren, S. J. 2009, MNRAS, 394, 675
Khargharia, J., Froning, C. S., & Robinson, E. L. 2010, ApJ, 716, 1105
Krivonos, R., Tsygankov, S., Revnivtsev, M., et al. 2010, A&A, 523, AA61
Krivonos, R., Tsygankov, S., Lutovinov, A., et al. 2012, A&A, 545, A27
Krühler, T., Küpcü Yoldas, A., Greiner, J., et al. 2008, ApJ, 685, 376
Kuulkers, E., Shaw, S. E., Paizis, A., et al. 2007, A&A, 466, 595
Lawrence, A., Warren, S. J., Almaini, O., et al. 2007, MNRAS, 379, 1599
Lawrence, A., Warren, S. J., Almaini, O., et al. 2012, yCat, 2314, 0
Lebrun, F., Leray, J. P., Lavocat, P., et al. 2003, A&A, 411, L141
Lund, N., Budtz-Jörgensen, C., Westergaard, N. J., et al. 2003, A&A, 411, L231
Lutovinov, A. A., Revnivtsev, M. G., Tsygankov, S. S., & Krivonos, R. A. 2013, MNRAS, 431, 327
Minniti, D., Lucas, P. W., Emerson, J. P., et al. 2010, NewA, 15, 433
Morrison, R., & McCammon, D. 1983, ApJ, 270, 119
Muno, M. P., Arabadjis, J. S., Baganoff, F. K., et al. 2004, ApJ, 613, 1179
Murdin, P., Jauncey, D. L., Lerche, I., et al. 1980, A&A, 87, 292
Ng, C., Díaz Trigo, M., Cadolle Bel, M., & Migliari, S. 2010, A&A, 522, A96
Nishiyama, S., Tamura, M., Hatano, H., et al. 2009, ApJ, 696, 1407
Nowak, M. A., Paizis, A., Rodriguez, J., et al. 2012, ApJ, 757, 143
Paizis, A., Mereghetti, S., Götz, D., et al. 2013, A&C, 1, 33
Paizis, A., Nowak, M., Chaty, S., et al. 2015, ATel, 7020
Predehl, P., & Schmitt, J. H. M. M. 1995, A&A, 293, 889
Revnivtsev, M., Lutovinov, A., Churazov, E., et al. 2008, A&A, 491, 209
Rieke, G. H., & Lebofsky, M. J. 1985, ApJ, 288, 618
Rodriguez, J., Bodaghee, A., Kaaret, P., et al. 2006, MNRAS, 366, 274
Rodriguez, J., Corbel, S., Caballero, I., et al. 2011, A&A, 533, L4
Rodriguez, J., Tomsick, J. A., & Bodaghee, A. 2010, A&A, 517, A14
Segreto, A., Cusumano, G., Ferrigno, C., et al. 2010, A&A, 510, A47
Shirey, R. E., Bradt, H. V., Levine, A. M., & Morgan, E. H. 1996, ApJL, 469, L21
Sidoli, L., Paizis, A., Bazzano, A., & Mereghetti, S. 2006, A&A, 460, 229
Skrutskie, M. F., Cutri, R. M., Stiening, R., et al. 2006, AJ, 131, 1163
Tendulkar, S. P., Bachetti, M., Tomsick, J. A., Chenevez, J., & Harrison, F. 2014, ATel, 6574
Tomsick, J. A., Bodaghee, A., Chaty, S., et al. 2012, ApJ, 754, 145
Wilms, J., Allen, A., & McCray, R. 2000, ApJ, 542, 914
Winkler, C., Courvoisier, T.J.-L., Di Cocco, G., et al. 2003, A&A, 411, L1
Winkler, C., Diehl, R., Ubertini, P., & Wilms, J. 2011, SSRv, 161, 149
Zurita Heras, J. A., Chaty, S., & Tomsick, J. A. 2009, A&A, 502, 787